Phosphorylation by CIPK23 regulates the high-affinity Mn transporter NRAMP1 in Arabidopsis

Thibault Kosuth, Alexandra Leskova, Reyes Ródenas, Gregory Vert, Curie Catherine, Loren Castaings

Phosphorylation by CIPK23 regulates the high-affinity Mn transporter NRAMP1 in Arabidopsis

Thibault Kosuth[1], Alexandra Leskova[1], Reyes Ródenas[2], Gregory Vert[2], Catherine Curie[1] & Loren Castaings[1]

[1] IPSiM, Univ Montpellier, CNRS, INRAE, Institut Agro, Montpellier, France

[2] Plant Science Research Laboratory (LRSV), UMR5546 CNRS/University of Toulouse 3, Auzeville Tolosane, France.

CORRESPONDANCE

Loren Castaings, IPSiM, 2 place Pierre Viala, 30060 Montpellier, France

Tel : +334 99 61 31 99

E-mail: loren.castaings@umontpellier.fr

KEY WORDS

Manganese, Transport, NRAMP1, CIPK23, Phosphorylation, kinase, *Arabidopsis thaliana*

ABBREVIATIONS

NRAMP1: Natural Resistance Associated Macrophage Protein 1

CIPK: CBL-Interacting Protein Kinase

CBL: Calcineurin B-like protein

CPK: Calcium-dependent Protein Kinase

AKT1: Arabidopsis Potassium Transporter 1

IRT1: Iron Transporter 1

LecRK-I9: Legume-like lectin receptor kinases I9

LUC: Luciferase

GFP: Green Fluorescent Protein

RFP: Red Fluorescent Protein

MBP: Maltose binding protein

GST: Glutathione S-Transferase

HA: Human influenza hemagglutinin tag

Cter: carboxyterminal

Nter: Amino terminal

GST-Nter: GST fused to the Nter fragment of NRAMP1

GST-Cter: GST fused to the Cter fragment of NRAMP1

ABSTRACT

Manganese (Mn) is essential for plants but is toxic when taken up in excess. To maintain Mn homeostasis, the root Mn transporter NRAMP1 cycles from the plasma membrane to endosomes upon phosphorylation. To identify the kinase involved, a split-luciferase screening was carried out between NRAMP1 and kinases of the CIPK family and identified CIPK23 as a partner of NRAMP1. The interaction was confirmed by split-mCitrine bimolecular fluorescence complementation and co-immunoprecipitation assays. *In vitro* phosphorylation assays pinpointed two CIPK23 target residues in NRAMP1, among which serine 20, important for endocytosis. Interestingly, Mn-induced internalization of NRAMP1 was unaffected by *cipk23* mutation suggesting a potential redundancy between CIPK23 and other kinase(s). How CIPK23 could regulate NRAMP1 in response to Mn availability is discussed.

INTRODUCTION

In plants, manganese (Mn) serves as a cofactor for numerous enzymes crucial for photosynthesis, reactive oxygen species detoxification, protein glycosylation, or cell wall components production. Mn deficiency generates therefore many cell disorders ultimately leading to poor growth of the plant, decreased fertility and susceptibility to pathogens [1]. Mn excess is also deleterious for plant cells as it triggers mismetallation of enzymes, excessive ROS production, accumulation of oxidized phenolic compounds in the apoplast, and competition with the uptake of other nutrients [2,3]. As a consequence, plants exposed to an excess of Mn eventually suffer important oxidative stress, impaired photosynthesis and secondary nutrient deficiencies [4,5].

Plants must therefore control Mn uptake in order to maintain Mn homeostasis and feed the Mn-dependent enzymes while avoiding toxicity. In Arabidopsis, Mn uptake is mainly ensured by two metal transporters, namely NRAMP1 and IRT1. NRAMP1 is responsible for the high-affinity Mn uptake [6], that allows plants to thrive when Mn availability is reduced. IRT1, beyond its essential function as the major high-affinity Fe transporter at the root surface [7], also contributes to Mn uptake under optimal conditions [8].

NRAMP1 and IRT1 activities are regulated by Mn availability to maintain proper Mn uptake. This is achieved mainly by post-translational regulation of these transporters. Indeed, they are both addressed at the plasma membrane when their metal substrates are becoming scarce in order to maximize their uptake, and internalized in endosomes when Mn is in excess to protect the cell from toxicity [9–11]. Internalization of NRAMP1 and IRT1 relies on clathrin-mediated endocytosis induced by post-translational modifications added to the cytosolic domains of the transporters [10–12]. IRT1 can sense excessive Mn through its cytosolic loop, which triggers its phosphorylation by the CBL-interacting kinase CIPK23 and subsequent ubiquitination by the ubiquitin ligase IDF1, promoting its targeting to the vacuole [10]. In the case of NRAMP1, internalization in response to Mn excess depends on the phosphorylation of serine (Ser) 20 since a phosphodead mutation of this residue prevents its endocytosis [11]. In addition, phosphorylation of threonine (Thr) 498 at the C-terminus of NRAMP1 by the calcium-activated protein kinases CPK21 and CPK23 kinases promotes its transport activity in response to Mn limitation [13].

The above-mentioned kinases responsible for Mn-dependent regulation of NRAMP1 and IRT1 belong to two different families of Ca^{2+}- activated kinases: the CPKs (Calcium-dependent

Protein Kinase), that can directly bind Ca^{2+} and phosphorylate their target, and CIPKs (CBL-interacting protein kinase), that do not directly bind Ca^{2+} and need activation by Ca^{2+}-bound CBL (Calcineurin B-like protein) prior to phosphorylate their target [14–16]. These kinases decode cytosolic Ca^{2+} oscillations triggered upon perception of a signal, such as Mn deficiency or excess, and relay it by phosphorylating their target effector proteins, eventually leading to a cellular response [13,17–19]. Among these kinases, the CBL-interacting protein kinase CIPK23 has emerged as a central hub in the regulation of root nutrients acquisition systems [20].

In the present work we have identified the CBL-interacting kinase CIPK23 as a new kinase able to phosphorylate the high-affinity Mn transporter NRAMP1, thus adding a new layer of complexity to the regulation of Mn uptake in Arabidopsis. We found that CIPK23 interacts with NRAMP1 and phosphorylates Ser20 and Ser499. Investigating the role played by CIPK23-mediated phosphorylation in the regulation of NRAMP1 under Mn excess led to the conclusion that CIPK23 may act redundantly with other kinases in that process.

MATERIALS AND METHODS

Plant material, growth conditions and Mn excess treatment

WT and T-DNA insertion Arabidopsis lines of the Columbia (Col-0) ecotype were used in this study. The *nramp1-1* line (SALK_053236) (*nramp1* in the text) and the transgenic line *nramp1-1 35S::NRAMP1-GFP* #8 (NRAMP1-GFP in the text) were described in previous studies [6,11]. The *cipk23-5* line (Salk_138057) (*cipk23* in the text) was previously described [21,22]. The double mutant *cbl1 cbl9* was previously described [23] and generated by crossing of the *cbl1* (SALK_110426) and *cbl9* (SALK_142774) lines [24]. The transgenic lines *cipk23-5 nramp1-1 35S::NRAMP1-GFP* (*cipk23 NRAMP1-GFP* in the text) and *cbl1 cbl9 nramp1-1 35S::NRAMP1-GFP* (*cbl1 cbl9 NRAMP1-GFP* in the text) were obtained by crossing the previously published *nramp1-1 35S::NRAMP1-GFP* #8 line with the *cipk23-5* and *cbl1 cbl9* mutants, respectively.

Transient expression in *Nicotiana benthamiana* leaves

A. tumefaciens GV3101 strains carrying the constructs of interest (including P19) were grown overnight and resuspended in infiltration buffer (10 mM $MgCl_2$; 10 mM MES [pH 5.6] and 150 µM acetosyringone) to a final OD_{600} of 0.1 each for split-LUC assay and 0.5 each for split-

mCitrine assay. Bacteria were co-incubated and then infiltrated in four-week-old *N. benthamiana* leaves.

Split-LUC assay

The Gateway® technology (Invitrogen) was used to clone the coding sequences of CIPK23 and CIPK20 into pDEST-nLUC^{GW} vector [25], and the coding sequences of NRAMP1 and AKT1 into pDEST-^{GW}cLUC and pDEST-cLUC^{GW} vectors respectively [25]. Combinations of Agrobacterium strains carrying these constructs were co-infiltrated in tobacco leaves. Leaf disks were harvested 72 h after infiltration and incubated 1 h in the dark with 1 mM luciferin in infiltration buffer. Luminescence intensity was measured by Victor microplate reader (Perkin Elmer Wallac Victor2 1420 Multilabel Counter). The mean of 3 reads was done for each leaf disk. Luminescence of 8 leaf disks from 2 different plants were measured for each combination of constructs. Luminescence intensity values were plotted relative to that of the positive control cLUC-AKT1/nLUC-CIPK23 combination set to 1.

Split-mCitrine assay

The Gateway® technology (Invitrogen) was used to clone mCitrine N-terminal (nCit) or C-terminal (cCit) fragments (residues 1 to 155 and 155 to 238, respectively) and the 2x35S promoter into p2R-P3 and p4-P1R donor vectors, respectively. The coding sequences without stop codons of NRAMP1, LecRK-I.9, CIPK23 and CIPK20 were cloned in pDONR207 vector and subcloned in 2X35S::GW-nCit and 2X35S::GW-cCit vectors, respectively. Combinations of Agrobacterium strains carrying these constructs were co-infiltrated in tobacco leaves. The mCitrine fluorescence imaging was performed 48 h after infiltration with an inverted Leica TCS SP8 confocal laser scanning microscope (25x water objective; 514 nm excitation, 525-580 nm detection). Chloroplast fluorescence was collected from 700 to 737 nm.

Root phenotyping experiment and Mn content quantification

Plants were grown vertically *in vitro* for 14 days under long days (23°C, 16h light/8 h dark, 65% RH) on sterile ½ MS medium containing 1% sucrose, 0.8% agar, and either 20 µM (standard) or 1 mM $MnSO_4$. Plates were scanned to allow primary root length (PRL) measurement using ImageJ. Shoots were harvested and rinsed 2 min in 10 mM EDTA. 8 to 20 shoots from the same genotype and growth condition were pooled, dried at 80°C for at least 2 days and mineralized in 7.5 % H_2O_2, 49 % HNO_3 at 85°C until complete disintegration.

Elemental analyses were performed by Micro Plasma Atomic Emission Spectroscopy (Agilent 4200 MP-AES) according to the manufacturer's recommendations.

Mn treatment of Arabidopsis roots, confocal imaging and fluorescence quantification

For imaging GFP fluorescence in Arabidopsis root cells, plants were grown one week under long days (21.5°C, 16h light/8 h dark, 65% RH) in a Mn-free ½ MS liquid medium (1% sucrose). Seedlings were then incubated in ½ MS Mn-free liquid medium for 1 h or in ½ MS containing 2 mM $MnSO_4$ for the amount of time indicated in the figure legend. The incubation media were supplemented with 100 µM of the translational inhibitor cycloheximide (Sigma Aldrich) in order to specifically observe the post-translational fate of NRAMP1-GFP proteins. Epidermal and cortical root cells from the division and elongation zone were imaged using an inverted Leica SP8 confocal microscope (40×/1.1 water objective; 488 nm excitation, 500–540 nm detection). The ratio of the plasma membrane over the intracellular signal intensity was calculated for individual cells by dividing the mean grey value of a segmented line (1-pixel wide) drawn along the plasma membrane by the mean grey value of the whole intracellular selected area on individual microscopic pictures, using ImageJ. For each time point, ratios of at least 10 different cells of 4 different plants were calculated.

Co-Immunoprecipitation and immunoblotting

The Gateway® technology (Invitrogen) was used to clone the coding sequences of CIPK23 and CBL1 in the pGWB5 and pB7RW62 vectors respectively. Combinations of Agrobacterium strains carrying these constructs and the pFP101-HA-NRAMP1 (described in [6]) were co-infiltrated in tobacco leaves. Infiltrated leaf samples were harvested 48 h after-infiltration and proteins were crosslinked before extraction. Transformed leaf samples were vacuumed 15min in 1X PBS 1 % formaldehyde. Crosslinking reaction was stopped by addition of 0.125 M Glycine. Total proteins (Inputs) were extracted from 1 g of crosslinked leaf tissue in 3 mL extraction buffer (50 mM Tris-HCl [pH 8]; 150 mM NaCl; 0,5 % Na Deoxycholate; 1 % Triton X-100; 0.1 % SDS; 5 mM DTT and 1 % Protease Inhibitor Cocktail for Plant Cell [Sigma]). HA-NRAMP1 or CIPK23-GFP proteins were immunopurified from total proteins with anti-HA and anti-GFP microbeads respectively (Miltenyi Biotec µMACS Isolation kit) according to the manufacturer's recommendations. Immunodetection of HA-NRAMP1, CIPK23-GFP and CBL1-RFP was performed as previously described [11] with the following antibodies respectively: anti-HA (5B1D10, 1:500, ThermoFisher), anti-GFP (JL-8, 1:4000, Clontech) and anti-RFP (6G6, 1:2000, Chromotek).

Production of recombinant proteins

The Gateway® technology was used to clone the coding sequences of CIPK23 and CIPK20 into the pKM596-MBP-GW vector. A stop codon was added by PCR to the coding sequences of NRAMP1 N-terminal domain (amino acids 1 to 45) which was then cloned in pDEST^{TM}15-GST-GW vector. pDEST^{TM}15-GST-Nter-S20,22,24A, pDEST^{TM}15-GST-Nter-S20A, pDEST^{TM}15-GST-Nter-S22A and pDEST^{TM}15-GST-Nter-S24A constructs were obtained similarly using mutated NRAMP1 coding sequences as previously described [11]. The coding sequences of NRAMP1 C-terminal domain (amino acids 493 to 532) was cloned in the pDEST^{TM}15-GST-GW vector. NRAMP1 C-terminal domains carrying point mutations to mutate Ser499 into alanine (S499A) or Ser503 and Ser506 into aspartic acids (S503,506D) were obtained by PCR site directed mutagenesis. These variants were fused to GST as well by cloning into pDEST^{TM}15-GST-GW.

E. coli BL21 strain carrying these constructs were grown until OD_{600} 0.3. Expression of the fusion proteins was induced for 3 h by addition of 0.3 mM final Isopropyl β-D-1 thiogalactoside. Cells were harvested, resuspended in column buffer (20 mM HEPES pH 7, 150 mM NaCl) and lysed by sonication. MBP- and GST- recombinant proteins were incubated 2 h with Amylose Resin^{TM} (New England BioLabs) and Agarose-glutathion Pierce™ (Thermo Scientific), respectively and eluted from the resin respectively with 10 mM maltose or 10 mM reduced L-gluthathione in column buffer.

In Vitro Phosphorylation Assay

10 µg of purified recombinant substrate proteins GST-Nter, Cter or mutated variants were incubated 3 h at 30°C with 5 µg of MBP-CIPK23 or MBP-CIPK20 in kinase reaction buffer (1.5 mM $MnSO_4$; 2 mM $CaCl_2$; 0.5 mM DTT; 0.1 mM cold ATP and 2 µCi [γ-32P] ATP) and heated at 55°C for 5 min in loading buffer. The proteins were separated by SDS-PAGE and gels were stained with Coomassie brilliant blue. Radioactivity was detected with a Typhoon^{TM} FLA 9000 imager (GE Healthcare). Band intensity quantification was done using ImageJ software.

RESULTS

NRAMP1 interacts with the kinase CIPK23

In order to identify candidate kinase(s) responsible for NRAMP1 phosphorylation in response to Mn excess, we carried out an interaction screening between NRAMP1 and members of the CIPK family. To that aim, we realized a split-luciferase assay (Split-LUC) in *Nicotiana benthamiana* leaves to test the interaction between NRAMP1 harboring the C-terminal part of the luciferase (cLUC) and 12 CIPKs chosen on the basis of their putative overlapping expression territories and fused to the N-terminal part of the luciferase (nLUC). We could detect strong luminescence signals for the interaction between NRAMP1 and either one of the kinases CIPK6, CIPK23, CIPK25 (Fig. S1). Among them, CIPK23 was of particular interest because of its role in the regulation of several nutrient transport systems, including the Fe/Mn transporter IRT1 [20]. Interaction between CIPK23 and NRAMP1 was compared to the positive control CIPK23/AKT1, which interaction was previously reported [26]. It led to a 2.5 stronger signal confirming the significance of the NRAMP1/CIPK23 interaction. The specificity of NRAMP1 interaction with CIPK23 was then validated using CIPK20 as a negative control which did interact with none of the transporters (Fig. 1A). Based on these results, we decided to focus on the interaction between NRAMP1 and CIPK23.

We further confirmed the interaction of NRAMP1 with CIPK23 by bimolecular fluorescence complementation using a split-mCitrine assay. Fluorescence of the mCitrine was recovered when NRAMP1 fused to the N-terminal part of the mCitrine (NRAMP1-nCit) was co-expressed in tobacco leaves with CIPK23 fused to the C-terminal part of the mCitrine (CIPK23-cCit). The fluorescent signal was observed at the plasma membrane and in dotted structures that likely represent endosomes (Fig. 1B). Knowing that NRAMP1 traffics between these two compartments [6,9,11], and that the mCitrine reconstitution is irreversible once formed, these results suggest that the interaction with CIPK23 may occur at one or both locations. Interaction was not detected with the negative controls CIPK20 and NRAMP1, and CIPK23 and LecRK-I.9, a plasma membrane receptor-like kinase involved in plant-pathogen interaction [27], highlighting the specificity of the BiFC interaction observed between NRAMP1 and CIPK23 (Fig. 1B).

We then tested the formation of a protein complex between NRAMP1, CIPK23 and CBL1, a calcium-binding protein known to activate CIPK23 *in vivo* [26]. To that aim, CIPK23-GFP and HA-NRAMP1 were expressed in tobacco leaf epidermis in the presence or in the absence of CBL1-RFP and immunoprecipitation experiments were performed using anti-GFP or anti-HA antibodies. Immunoblot analysis on the immunoprecipitated proteins revealed that CIPK23-GFP was recovered from the HA-NRAMP1 protein complex and reciprocally (Fig. 1C). These

data further confirm our observations that CIPK23 and NRAMP1 interact *in vivo*. We then checked if the presence of CBL1 affected the interaction between NRAMP1 and CIPK23. Despite the fact that CBL1-RFP could be pulled down with CIPK23-GFP and/or HA-NRAMP1, its presence was not mandatory for the binding between NRAMP1 and CIPK23 since CIPK23-GFP and HA-NRAMP1 could co-precipitate in absence of CBL1-RFP (Fig. 1C). This suggests that either endogenous CBLs from tobacco cells can substitute to CBL1-RFP to promote interaction between CIPK23 and NRAMP1 or that CBL1 is not essential for such interaction.

Altogether these data support an interaction between the Mn transporter NRAMP1 and the protein kinase CIPK23 *in planta*.

NRAMP1 Ser20 and Ser499 are phosphorylated by CIPK23

As we have shown that CIPK23 interacts with NRAMP1, we then tested if it can phosphorylate the transporter on its N- and C-terminal cytosolic domains by performing *in vitro* phosphorylation assays (Fig 2 and Fig S2). To that aim, we combined purified MBP-CIPK23 with either N- or C-terminal parts of NRAMP1 fused to the GST tag (GST-Nter and GST-Cter, respectively) in the presence of ^{32}P-radiolabeled ATP (Fig. 2A). A radioactive signal corresponding to MBP-CIPK23 autophosphorylation was detected, attesting of the functionality of the purified kinase. Interestingly, both GST-Nter and GST-Cter fragments of NRAMP1 were radiolabeled, indicating that both N- and C-termini of NRAMP1 can be phosphorylated by CIPK23. When incubated with MBP-CIPK20 however, only CIPK20 autophosphorylation was detected and neither GST-Nter nor GST-Cter fragments were phosphorylated (Fig. 2A). These results indicate that one or several residues of NRAMP1 N- and C-termini are specifically phosphorylated by CIPK23 *in vitro*.

CIPK23 belongs to the Ser/Thr class of kinases that exclusively phosphorylate Ser and Thr residues of their target proteins. NRAMP1 N- and C-terminal tails contain several Ser and Thr residues, some of which playing important roles in the regulation of NRAMP1 [11,13]. We have previously shown that phosphorylation of Ser20 at the N-terminus of NRAMP1 is required for its endocytosis under Mn excess conditions [11]. This prompted us to test if CIPK23 also phosphorylates Ser20 and the nearby Ser22 and Ser24. We therefore generated point mutation variants of GST-Nter for Ser20, Ser22 and Ser24 and assessed their phosphorylation *in vitro* in the presence of CIPK23 (Fig. 2B). When all Ser20, 22, 24 were mutated (Nter S20, 22, 24A),

phosphorylation of the NRAMP1 Nter part was completely abolished, indicating that one or several of these residues are phosphorylated by CIPK23. We then tested individual point mutations of Ser20, Ser22 or Ser24 and we could detect a significant decrease in phosphorylation only when Ser20 was mutated (Fig. 2B). This result identifies Ser20 as a major target of CIPK23 in the N terminal part of NRAMP1.

We have shown that CIPK23 is also able to phosphorylate the C-terminal domain of NRAMP1 (Fig. 2A). We therefore generated point mutation variants of GST-Cter in which either both Ser503 and Ser506 or Ser499 were replaced by non-phosphorylatable residues. Phosphorylation of GST-Cter by CIPK23 was unaffected by the S503,506D mutation, indicating that these two residues are not targets of CIPK23 (Fig. 2B). Mutation of Ser499 on the contrary completely abolished the phosphorylation of GST-Cter by CIPK23 (Fig. 2B). This result establishes that Ser499 is the only target of CIPK23 on the C terminal cytosolic region of NRAMP1.

Together these data indicate that the interaction of CIPK23 with NRAMP1 leads to phosphorylation of NRAMP1 and identify Ser20 and Ser499, located in NRAMP1 N- and C-terminal domains respectively, as the main residues phosphorylated by CIPK23.

The CIPK23-CBL1/9 module is not mandatory for Mn-induced endocytosis of NRAMP1

Based on our data showing that the Ser20 of NRAMP1 is phosphorylated by the kinase CIPK23, we asked whether this kinase could contribute to the plant response to Mn excess by provoking NRAMP1 endocytosis. Since NRAMP1 stabilization at the plasma membrane leads to hypersensitivity to Mn, we assessed the tolerance of the *cipk23* mutant to Mn excess, which would potentially reflect a defect in NRAMP1 endocytosis in this background. We exposed *cipk23* mutant and WT plants to 1mM Mn *in vitro* and monitored root growth inhibition and Mn accumulation in leaves (Fig. 3). While *cipk23* mutant displayed no specific phenotype under standard Mn concentration, it showed a significant decrease in primary root length when exposed to high Mn, notably stronger than the one observed in the WT (Fig. 3A). Moreover, *cipk23* mutant accumulated more Mn in leaves than the WT when grown under Mn excess conditions (Fig. 3B and C). These results indicate that the *cipk23* mutant accumulates excessive amounts of Mn leading to its hypersensitivity to Mn excess and prompted us to search for a defect of Mn-induced internalization of NRAMP1 in the mutant.

To that aim, the *cipk23* mutation was introgressed into a NRAMP1-GFP overexpressor line (described in [11]) and NRAMP1-GFP membrane dynamics in root cells was monitored in the mutant background. The kinetics of Mn-induced internalization of NRAMP1-GFP was followed in this line by confocal microscopy after 1h and 2h of Mn treatment (Fig. 4A and B). As previously reported [11], when the control NRAMP1-GFP line was exposed to elevated Mn, the plasma membrane localization of the GFP fluorescent signal progressively shifted to endosomal compartments, reflecting NRAMP1-GFP endocytosis. In the *cipk23* mutant background, NRAMP1-GFP internalization in response to Mn remained largely unchanged (*cipk23* NRAMP1 Fig. 4A) and showed similar kinetics as the one observed in the wild-type control (Fig. 4B). This result indicates that the absence of CIPK23 does not impair NRAMP1-GFP internalization in the NRAMP1-GFP overexpressor line. To overcome potential redundancy among CIPKs in NRAMP1 Mn-induced endocytosis, we decided to investigate the Mn sensitivity of a *cbl1cbl9* double mutant impaired in the activation of several plasma membrane CIPKs. When exposed to toxic Mn amounts, the *cbl1cbl9* mutant exhibited root growth inhibition and Mn overaccumulation that were even stronger than that of the *cipk23* mutant, supporting our hypothesis that several CIPKs may contribute to NRAMP1 regulation (Fig. 3). This observation prompted us to follow NRAMP1-GFP dynamics in the *cbl1cbl9* double mutant. We introgressed *cbl1cbl9* double mutations in the NRAMP1-GFP line and challenged *cbl1 cbl9* NRAMP1-GFP plants with an excess of Mn in order to trigger NRAMP1-GFP internalization. In this double mutant background, NRAMP1-GFP was internalized with no detectable change in kinetics compared to its wild-type counterpart (Fig. 4C and D). This result indicates that the absence of CIPK23 or CBL1/CBL9 is not sufficient to block Mn-induced endocytosis of NRAMP1, suggesting that other kinases may compensate for the lack of their activities.

DISCUSSION

In the present work we showed that the high-affinity Mn transporter NRAMP1 interacts with and is phosphorylated by the calcium responsive kinase CIPK23. We localized NRAMP1 and CIPK23 complexes at the plasma membrane and/or in endosomes by BiFC. Whether NRAMP1 only transits by endosomes or whether it acts there as a Mn transporter and interacts with CIPK23 in that compartment remains to be investigated.

We identified Ser20 in the N-terminal cytosolic domain of the transporter as a target residue of the kinase. Since we previously showed that phosphorylation of Ser20 is required for NRAMP1 internalization under Mn excess [11], we investigated the role of CIPK23 and of CBL1 and CBL9 in NRAMP1 endocytosis in response to exposure to toxic Mn levels. Strikingly, the absence of either CIPK23 or both CBL1 and CBL9 did not significantly perturbed Mn-induced internalization of NRAMP1-GFP. This result led us to the hypothesis that several kinases may act redundantly to promote Ser20 phosphorylation and trigger NRAMP1 endocytosis. In support of our hypothesis, Fu *et al*. [13] have shown that, in addition to Thr498, the calcium-dependent protein kinases CPK21 and CPK23 can also phosphorylate Ser20. However, the authors reported that Mn-induced NRAMP1 endocytosis was unaltered in a *cpk21 cpk23* mutant, similar to what we observed in the *cipk23* mutant. Following NRAMP1 dynamics in a *cpk21 cpk23 cipk23* triple mutant or in a *cpk21 cpk23 cbl1 cbl9* quadruple mutant may clarify whether a functional redundancy exists among these kinases from different families in triggering Mn-induced NRAMP1 internalization.

Similar to what we describe here, Zhang *et al*. [28] have recently also reported NRAMP1 phosphorylation by CIPK23 on Ser20. Unlike our study however, they could show that Mn-induced internalization of NRAMP1-GFP is abolished in *cipk23* and *cbl1 cbl9* mutant backgrounds. Discrepancy between the two studies concerning the impact of knocking out CIPK23 on NRAMP1 dynamics may come from the use of different NRAMP1-GFP expressing lines. Indeed, while we investigated NRAMP1-GFP trafficking in a 35S overexpressor line, Zhang and colleagues used NRAMP1 native promoter to drive NRAMP1-GFP expression. We therefore cannot completely rule out that an overaccumulation of NRAMP1-GFP protein may hinder the contribution of CIPK23 and CBL1/9 to NRAMP1 internalization. This is however unexpected given that this line was previously used to establish NRAMP1 internalization in response to Mn [11]. In order to avoid potential artifacts originating from the use of transgenic lines and reporter protein fusions, immunostaining of native NRAMP1 protein in root cells of WT, *cipk23* and *cbl1 cbl9* mutant plants exposed to Mn excess may help to clarify this point.

In addition to Ser20, we identified Ser499 as the main target of CIPK23 in the C-terminal domain of NRAMP1. Interestingly, next to Ser499, Thr498 was shown to enhance NRAMP1 activity when phosphorylated by the kinases CPK21/CPK23 [13] and was reported recently as also phosphorylated by CIPK23 [28]. If the exact function of Ser499 phosphorylation is not yet known, two hypotheses can be proposed: Ser499 phosphorylation could (i) act in synergy with Thr498 phosphorylation and further enhance NRAMP1 activity or (ii) prevent Thr498

phosphorylation and downregulate NRAMP1 activity. Further work will be needed to find out if Thr498 and Ser499 phosphorylations are mutually exclusive or whether they can occur concomitantly and act in concert.

Striking is the fact that CIPK23 seems to regulate the two major Mn transporters at the plasma membrane NRAMP1 and IRT1 ([10,28] and the present work). This attests of the central role of this kinase in the control of Mn entry within the cell. We and others [10,28] have shown that *cipk23* and *cbl1 cbl9* are sensitive to Mn excess confirming their incapacity to control Mn entry in the plant. Given that NRAMP1 and IRT1 contribute to Mn acquisition probably with different affinities, it would be interesting to further investigate the contribution of each of these transporters in the Mn hypersensitive phenotype of the mutants and more generally in the cellular response to Mn excess.

ACKNOWLEDGMENTS

We thank Dr. Tou Cheu Xiong (IPSIM, Montpellier) for providing cDNA constructs for several CIPKs, Léna Laury for her help with Split-LUC experiments and Sandrine Chay from "service d'Analyses Multi-Elementaires" (SAME) from IPSiM (Univ Montpellier, INRAE, CNRS, Institut Agro, Montpellier) for Mn quantifications We acknowledge the imaging facility MRI and TRI, members of the national infrastructure France-BioImaging infrastructure supported by the French National Research Agency (ANR-10-INBS-04, «Investments for the future").

AUTHOR CONTRIBUTIONS

T.K, A.L, R.R performed the experiments. T.K and L.C analyzed the data. C.C and L.C designed and supervised the study. T.K and L.C wrote the manuscript. A.L, R.R, G.V and C.C revised the manuscript.

FUNDING

Work was funded by the Agence Nationale pour la Recherche through the ANR grant DEFIMAN (ANR-19-CE20-0009, to C.C) and NUTRISENSE (ANR-21-CE20-0046, to G.V.), by the Centre National de la Recherche Scientifique. L.C. and T.K. were supported by the University of Montpellier (France), and R.R. by a postdoctoral fellowship from the Alfonso Martín Escudero Foundation. A.L, G.V and C.C were supported by the Centre National de la Recherche Scientifique.

DATA AVAILABILITY

All data described are available in the article and its Supporting Information.

CONFLICT OF INTEREST

The authors declare that they have no conflicts of interest with the contents of this article.

REFERENCES

1 Marschner H & Marschner P (eds.) (2012) *Marschner's mineral nutrition of higher plants*, 3rd ed Elsevier/Academic Press, London ; Waltham, MA.

2 Goulding KWT (2016) Soil acidification and the importance of liming agricultural soils with particular reference to the United Kingdom. *Soil Use and Management* **32**, 390–399.

3 Li J, Jia Y, Dong R, Huang R, Liu P, Li X, Wang Z, Liu G & Chen Z (2019) Advances in the Mechanisms of Plant Tolerance to Manganese Toxicity. *International Journal of Molecular Sciences* **20**, 5096.

4 Horst WJ (1988) The Physiology of Manganese Toxicity. In *Manganese in Soils and Plants: Proceedings of the International Symposium on 'Manganese in Soils and Plants' held at the Waite Agricultural Research Institute, The University of Adelaide, Glen Osmond, South Australia, August 22–26, 1988 as an Australian Bicentennial Event* (Graham RD, Hannam RJ, & Uren NC, eds), pp. 175–188. Springer Netherlands, Dordrecht.

5 de Varennes A, Carneiro JP & Goss MJ (2001) Characterization of Manganese Toxicity in Two Species of Annual Medics. *Journal of Plant Nutrition* **24**, 1947–1955.

6 Cailliatte R, Schikora A, Briat J-F, Mari S & Curie C (2010) High-affinity manganese uptake by the metal transporter NRAMP1 is essential for Arabidopsis growth in low manganese conditions. *Plant Cell* **22**, 904–917.

7 Vert G, Grotz N, Dédaldéchamp F, Gaymard F, Guerinot ML, Briat J-F & Curie C (2002) IRT1, an Arabidopsis transporter essential for iron uptake from the soil and for plant growth. *Plant Cell* **14**, 1223–1233.

8 Castaings L, Caquot A, Loubet S & Curie C (2016) The high-affinity metal Transporters NRAMP1 and IRT1 Team up to Take up Iron under Sufficient Metal Provision. *Sci Rep* **6**, 37222.

9 Agorio A, Giraudat J, Bianchi MW, Marion J, Espagne C, Castaings L, Lelièvre F, Curie C, Thomine S & Merlot S (2017) Phosphatidylinositol 3-phosphate–binding protein AtPH1 controls the localization of the metal transporter NRAMP1 in Arabidopsis. *Proc Natl Acad Sci U S A* **114**, E3354–E3363.

10 Dubeaux G, Neveu J, Zelazny E & Vert G (2018) Metal Sensing by the IRT1 Transporter-Receptor Orchestrates Its Own Degradation and Plant Metal Nutrition. *Molecular Cell* **69**, 953-964.e5.

11 Castaings L, Alcon C, Kosuth T, Correia D & Curie C (2021) Manganese triggers phosphorylation-mediated endocytosis of the Arabidopsis metal transporter NRAMP1. *Plant J* **106**, 1328–1337.

12 Barberon M, Dubeaux G, Kolb C, Isono E, Zelazny E & Vert G (2014) Polarization of IRON-REGULATED TRANSPORTER 1 (IRT1) to the plant-soil interface plays crucial role in metal homeostasis. *Proc Natl Acad Sci U S A* **111**, 8293–8298.

13 Fu D, Zhang Z, Wallrad L, Wang Z, Höller S, Ju C, Schmitz-Thom I, Huang P, Wang L, Peiter E, Kudla J & Wang C (2022) Ca2+-dependent phosphorylation of NRAMP1 by CPK21 and CPK23 facilitates manganese uptake and homeostasis in Arabidopsis. *Proc Natl Acad Sci U S A* **119**, e2204574119.
14 Batistič O & Kudla J (2009) Plant calcineurin B-like proteins and their interacting protein kinases. *Biochimica et Biophysica Acta (BBA) - Molecular Cell Research* **1793**, 985–992.
15 Shi S, Li S, Asim M, Mao J, Xu D, Ullah Z, Liu G, Wang Q & Liu H (2018) The Arabidopsis Calcium-Dependent Protein Kinases (CDPKs) and Their Roles in Plant Growth Regulation and Abiotic Stress Responses. *International Journal of Molecular Sciences* **19**.
16 Kudla J, Becker D, Grill E, Hedrich R, Hippler M, Kummer U, Parniske M, Romeis T & Schumacher K (2018) Advances and current challenges in calcium signaling. *New Phytologist* **218**, 414–431.
17 Saito S & Uozumi N (2020) Calcium-Regulated Phosphorylation Systems Controlling Uptake and Balance of Plant Nutrients. *Front Plant Sci* **11**, 44.
18 Dong Q, Bai B, Almutairi BO & Kudla J (2021) Emerging roles of the CBL-CIPK calcium signaling network as key regulatory hub in plant nutrition. *Journal of Plant Physiology* **257**, 153335.
19 Verma P, Sanyal SK & Pandey GK (2021) Ca2+–CBL–CIPK: a modulator system for efficient nutrient acquisition. *Plant Cell Rep* **40**, 2111–2122.
20 Ródenas R & Vert G (2021) Regulation of Root Nutrient Transporters by CIPK23: "One Kinase to Rule Them All." *Plant Cell Physiol* **62**, 553–563.
21 Nieves-Cordones M, Caballero F, Martínez V & Rubio F (2012) Disruption of the Arabidopsis thaliana inward-rectifier K+ channel AKT1 improves plant responses to water stress. *Plant Cell Physiol* **53**, 423–432.
22 Ragel P, Ródenas R, García-Martín E, Andrés Z, Villalta I, Nieves-Cordones M, Rivero RM, Martínez V, Pardo JM, Quintero FJ & Rubio F (2015) The CBL-Interacting Protein Kinase CIPK23 Regulates HAK5-Mediated High-Affinity K+ Uptake in Arabidopsis Roots. *Plant Physiol* **169**, 2863–2873.
23 Cheong YH, Pandey GK, Grant JJ, Batistic O, Li L, Kim B-G, Lee S-C, Kudla J & Luan S (2007) Two calcineurin B-like calcium sensors, interacting with protein kinase CIPK23, regulate leaf transpiration and root potassium uptake in Arabidopsis. *The Plant Journal* **52**, 223–239.
24 Xu J, Li H-D, Chen L-Q, Wang Y, Liu L-L, He L & Wu W-H (2006) A protein kinase, interacting with two calcineurin B-like proteins, regulates K+ transporter AKT1 in Arabidopsis. *Cell* **125**, 1347–1360.
25 Gehl C, Kaufholdt D, Hamisch D, Bikker R, Kudla J, Mendel RR & Hänsch R (2011) Quantitative analysis of dynamic protein–protein interactions in planta by a floated-leaf luciferase complementation imaging (FLuCI) assay using binary Gateway vectors. *The Plant Journal* **67**, 542–553.
26 Li L, Kim B-G, Cheong YH, Pandey GK & Luan S (2006) A Ca(2)+ signaling pathway regulates a K(+) channel for low-K response in Arabidopsis. *Proc Natl Acad Sci U S A* **103**, 12625–12630.
27 Balagué C, Gouget A, Bouchez O, Souriac C, Haget N, Boutet-Mercey S, Govers F, Roby D & Canut H (2016) The Arabidopsis thaliana lectin receptor kinase LecRK-I.9 is required for full resistance to Pseudomonas syringae and affects jasmonate signalling. *Mol Plant Pathol* **18**, 937–948.

28 Zhang Z, Fu D, Xie D, Wang Z, Zhao Y, Ma X, Huang P, Ju C & Wang C (2023) CBL1/9–CIPK23–NRAMP1 axis regulates manganese toxicity. *New Phytologist* **239**, 660–672.

FIGURE LEGENDS

Fig.1: CIPK23 and NRAMP1 interact

(A) Relative luminescence in arbitrary units (A.U) obtained by Split-LUC assay between nLUC-CIPK23 and NRAMP1-cLUC. Luminescence values were normalized relative to the control interaction cLUC-AKT1/nLUC-CIPK23. The cLUC-AKT1/nLUC-CIPK20 combination was used as a negative control. Errors bars represent ± SD of the mean (n = 8). Different letters indicate significant differences between conditions (one-way ANOVA, Tukey HSD post-test, $p < 0.05$).

(B) Confocal images of a split-mCitrine assay between NRAMP1 and CIPK23. NRAMP1-nCit and CIPK23-cCit (top lane), NRAMP1-nCit and CIPK20-cCit (middle lane) and LecRK-I9-nCit and CIPK23-cCit (bottom lane). Yellow, mCitrine fluorescence. Cyan, chloroplasts auto-fluorescence. Scale bars, 10 µm.

(C) Co-immunoprecipitation assay of CIPK23-GFP, HA-NRAMP1 and CBL1-RFP in tobacco leaves. IPs, immunoprecipitations; IB, immunoblotting.

Fig. 2: CIPK23 phosphorylates NRAMP1 on Ser20 and Ser499

(A) *In vitro* phosphorylation assay of N-terminal (GST-Nter) and C-terminal regions (GST-Cter) of NRAMP1 by MBP-CIPK23 or MBP-CIPK20.

(B) Identification of the phosphorylation target sites of CIPK23 by *in vitro* phosphorylation assay of mutated N-terminal (GST-Nter) and C-terminal regions (GST-Cter) of NRAMP1. Intensity ratios between Autorad and CBB signals were calculated for GST-Nter variants and GST-Cter variants and expressed relatively to those of the GST-Nter or GST-Cter, respectively. CBB, Coomassie brilliant blue staining. Autorad, autoradiography.

Fig. 3: *cipk23* and *cbl1 cbl9* mutants are sensitive to Mn excess

(A) Primary root length (PRL) of WT, *cipk23*, *cbl1 cbl9* seedlings grown on 20 µM Mn (standard) or 1 mM Mn agar plates for 14 days. Error bars represent ± SD of the mean (n = 25 to 30).

(B) and (C) Shoot Mn content of WT, *cipk23*, *cbl1 cbl9* seedlings grown on agar plates for 14 days with 20 µM Mn (standard) or 1 mM Mn, respectively. (B) and (C) share legends. Error bars represent ± SD of the mean (n = 3).

An asterisk indicates significant difference with the WT (Student T-test, * $p < 0.01$, ** $p<0.005$, *** $p<0.001$). ns indicates non-significant difference with the WT (Student T-test, $p > 0.05$).

Fig. 4: Mn-induced endocytosis in *cipk23* and *cbl1 cbl9* mutants

(A) Confocal images of root cells from Mn-starved *NRAMP1-GFP* and *cipk23 NRAMP1-GFP* seedlings treated with 2 mM $MnSO_4$ for 0 h, 1 h or 2 h. Scale bars, 10µm.

(B) Quantification of the ratio between NRAMP1-GFP plasma membrane and intracellular signal intensities in *NRAMP1-GFP* and *cipk23 NRAMP1-GFP* plants grown as in (A).

(C) Confocal images of root cells from Mn-starved *NRAMP1-GFP* and *cbl1 cbl9 NRAMP1-GFP* seedlings treated with 2 mM $MnSO_4$ for 0 h, 1 h or 2 h. Scale bars, 10µm.

(D) Quantification of the ratio between NRAMP1-GFP plasma membrane and intracellular signal intensities in *NRAMP1-GFP* and *cbl1 cbl9 NRAMP1-GFP* plants grown as in (C).

In (B) and (D), error bars represent ± SD of the mean (n = 40 cells) and different letters indicate significant differences between conditions (two-way ANOVA, Tukey HSD post-test, $p < 0.05$).

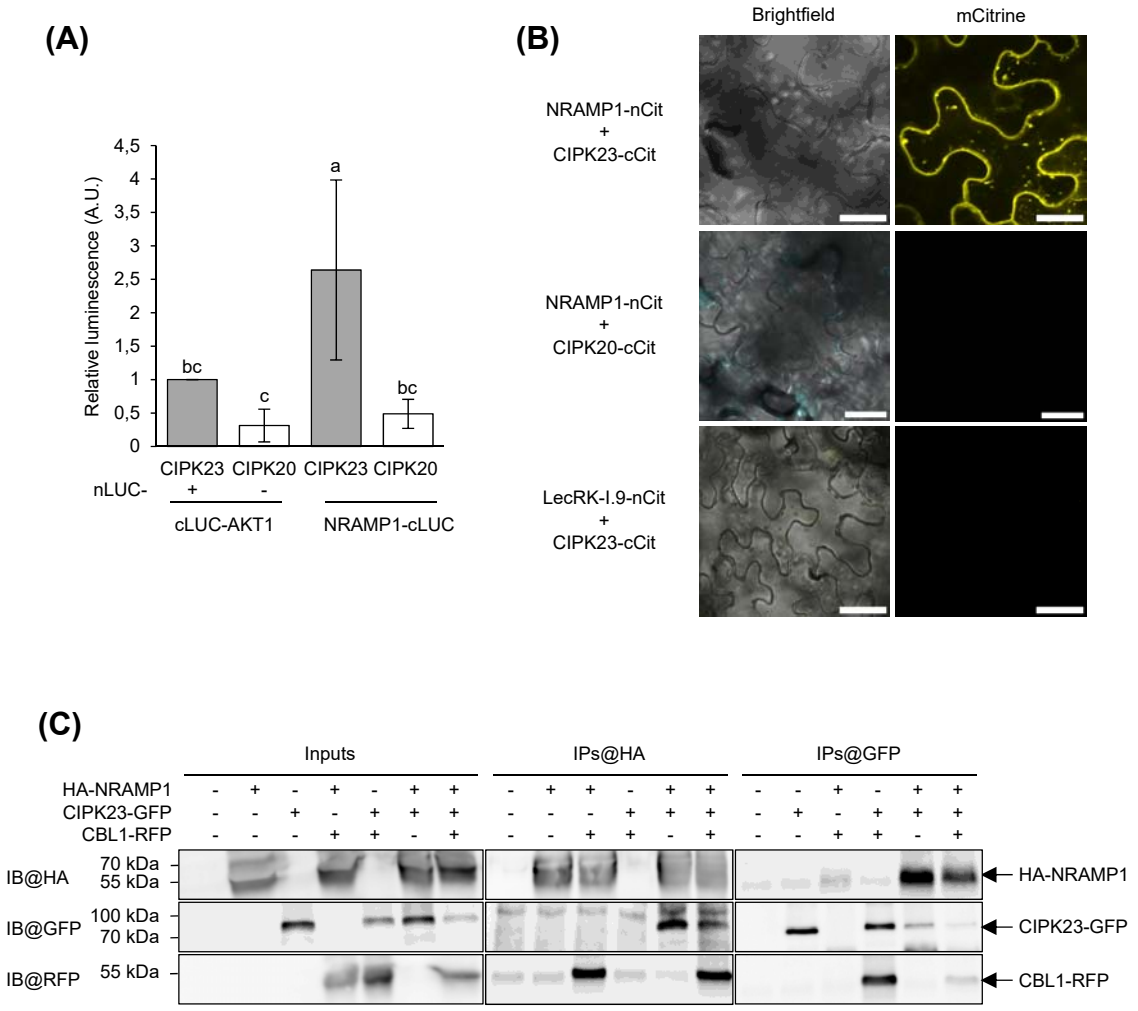

Fig.1 : CIPK23 and NRAMP1 interact.

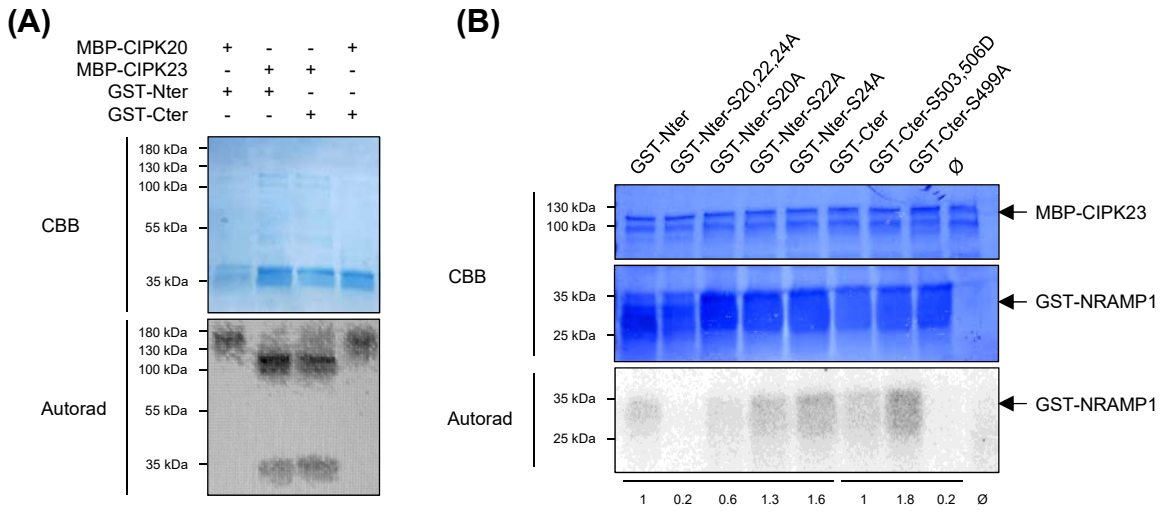

Fig. 2 : CIPK23 phosphorylates NRAMP1 on Ser20 and Ser499.

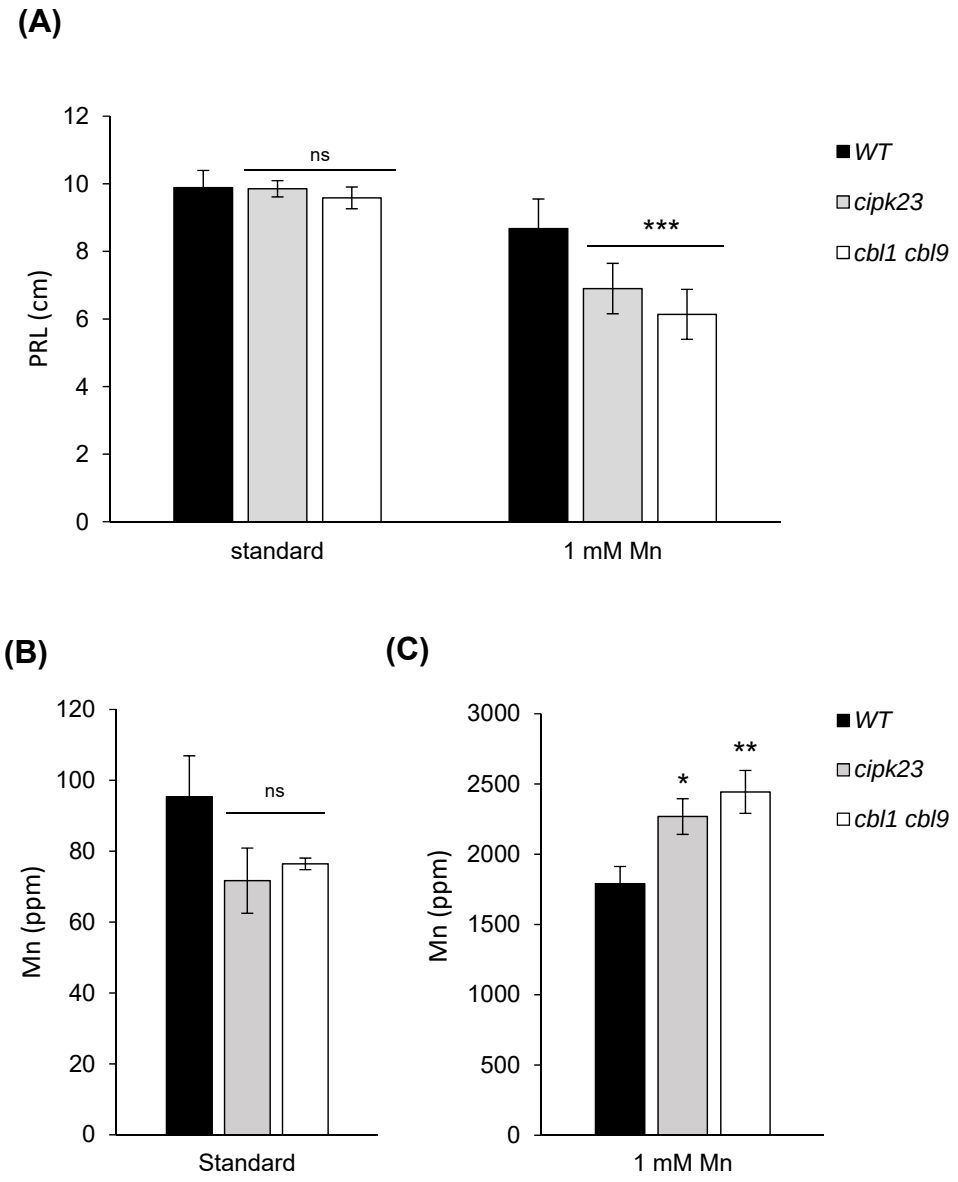

Fig. 3 : *cipk23* and *cbl1 cbl9* mutants are sensitive to Mn excess.

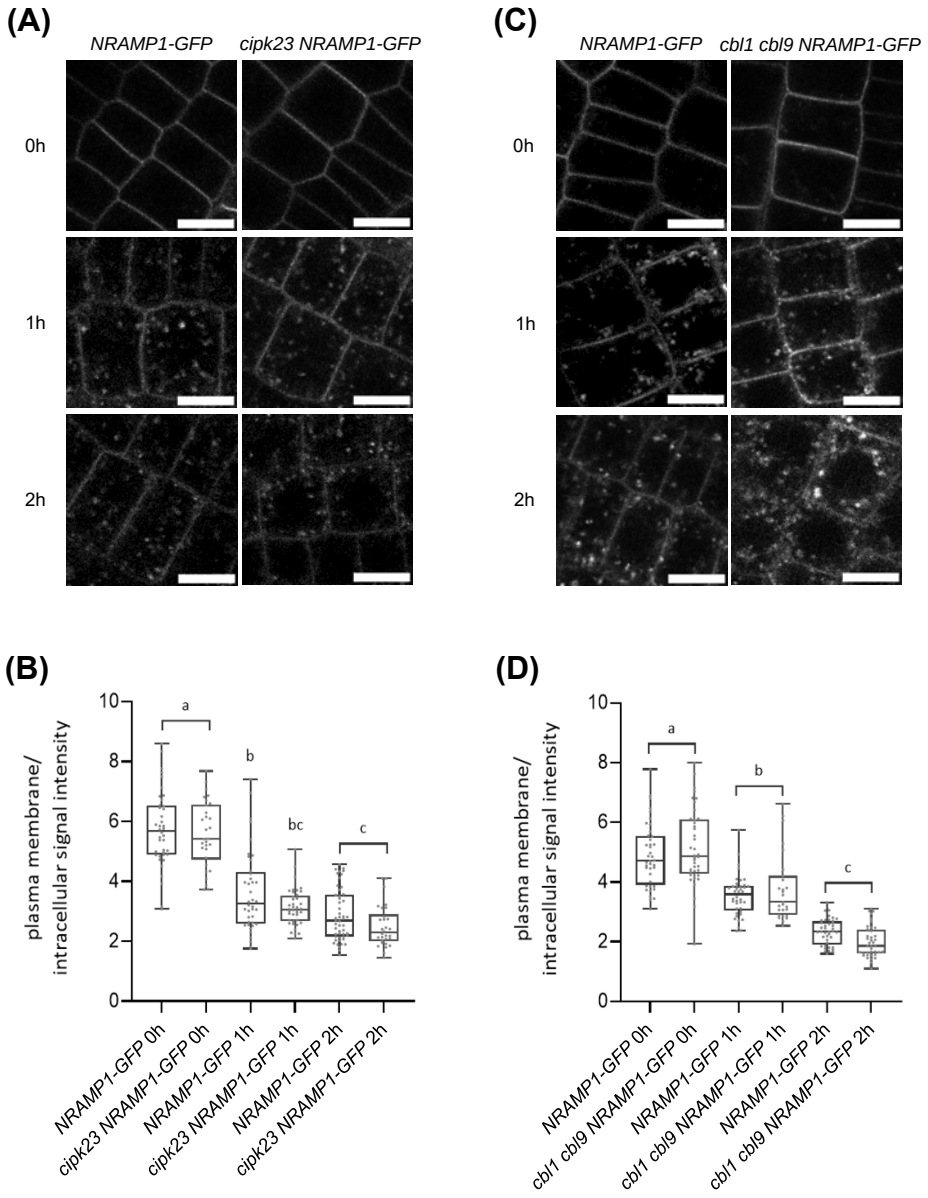

Fig. 4 : Mn-induced endocytosis in *cipk23* and *cbl1 cbl9* mutants.

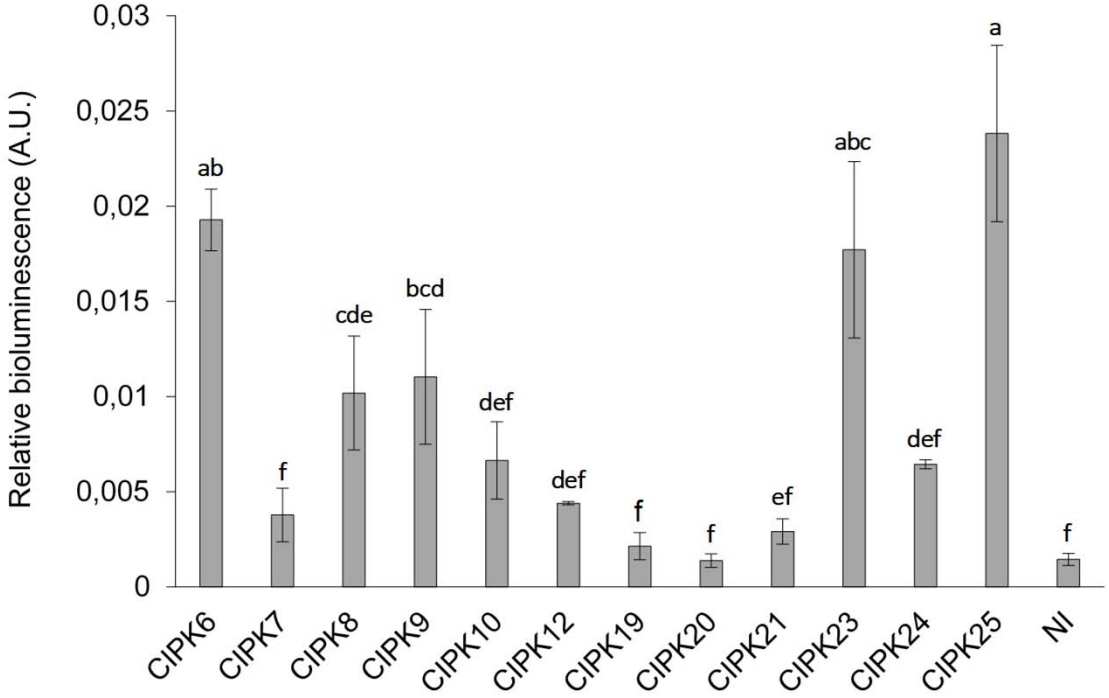
Relative bioluminescence (A.U.)
0,03
0,025
0,02
0,015
0,01
0,005
0
ab
f
cde
bcd
def
def
f
f
ef
abc
def
a
f
CIPK6
CIPK7
CIPK8
CIPK9
CIPK10
CIPK12
CIPK19
CIPK20
CIPK21
CIPK23
CIPK24
CIPK25
NI

Figure S1

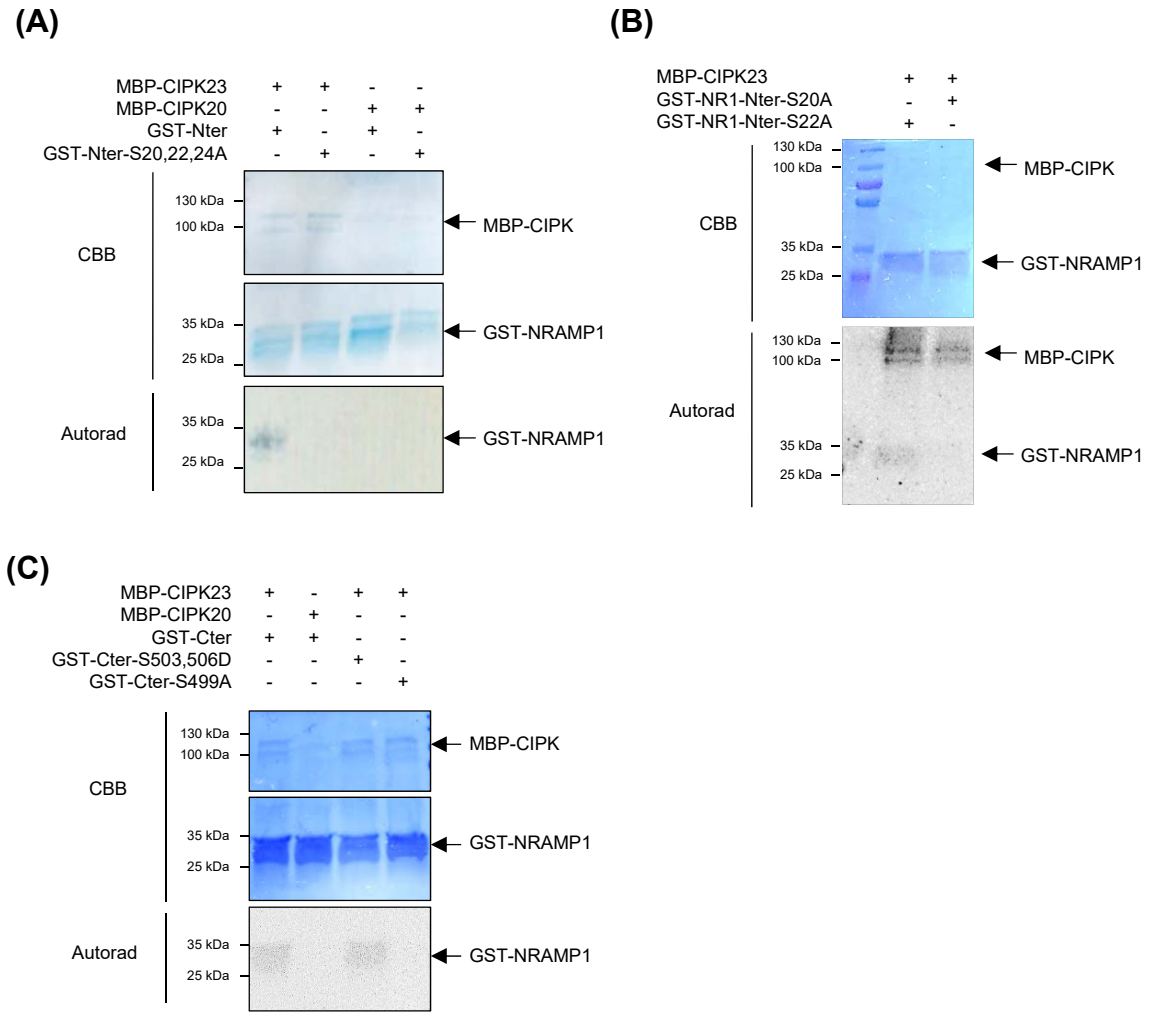
(A)
MBP-CIPK23 + + - -
MBP-CIPK20 - - + +
GST-Nter + - + -
GST-Nter-S20,22,24A - + - +
CBB
130 kDa
100 kDa
MBP-CIPK
35 kDa
25 kDa
GST-NRAMP1
Autorad
35 kDa
25 kDa
GST-NRAMP1
(B)
MBP-CIPK23 + +
GST-NR1-Nter-S20A - +
GST-NR1-Nter-S22A + -
CBB
130 kDa
100 kDa
MBP-CIPK
35 kDa
25 kDa
GST-NRAMP1
Autorad
130 kDa
100 kDa
MBP-CIPK
35 kDa
25 kDa
GST-NRAMP1
(C)
MBP-CIPK23 + - + +
MBP-CIPK20 - + - -
GST-Cter + + - -
GST-Cter-S503,506D - - + -
GST-Cter-S499A - - - +
CBB
130 kDa
100 kDa
MBP-CIPK
35 kDa
25 kDa
GST-NRAMP1
Autorad
35 kDa
25 kDa
GST-NRAMP1

Figure S2

SUPPORTING INFORMATION FOR

Phosphorylation by CIPK23 regulates the high-affinity Mn transporter NRAMP1 in Arabidopsis

Thibault Kosuth, Alexandra Leskova, Reyes Ródenas, Gregory Vert, Catherine Curie & Loren Castaings

Material included

Supporting materials and methods

Supporting Figure S1

Supporting Figure S2

Supporting materials and methods

Split-LUC assay

The Gateway® technology (Invitrogen) was used to generate the split-LUC expression vectors. The coding sequences of CIPKs were cloned in pDEST-nLUC^{GW} vector carrying an internal GFP cassette to evaluate efficiency transformation (26) and the coding sequences of NRAMP1 in pDEST-^{GW}cLUC (26). Combinations of Agrobacterium strains carrying these constructs were co-infiltrated in tobacco leaves (see Tobacco infiltration methods in the main text). Leaf disks were harvested 72h after infiltration and incubated 1h in the dark with 1 mM luciferin in infiltration buffer. Luminescence intensity as well as GFP fluorescence intensity were measured by the CLARIOStar® microplate reader (BMG labtech). The mean of 3 reads was made for each leaf disk and 3 leaf disks from 2 different plants were measured per combination of constructs. Relative luminescence values were obtained by dividing luminescence intensity value by the GFP intensity value for each leaf disc.

Supporting Figures

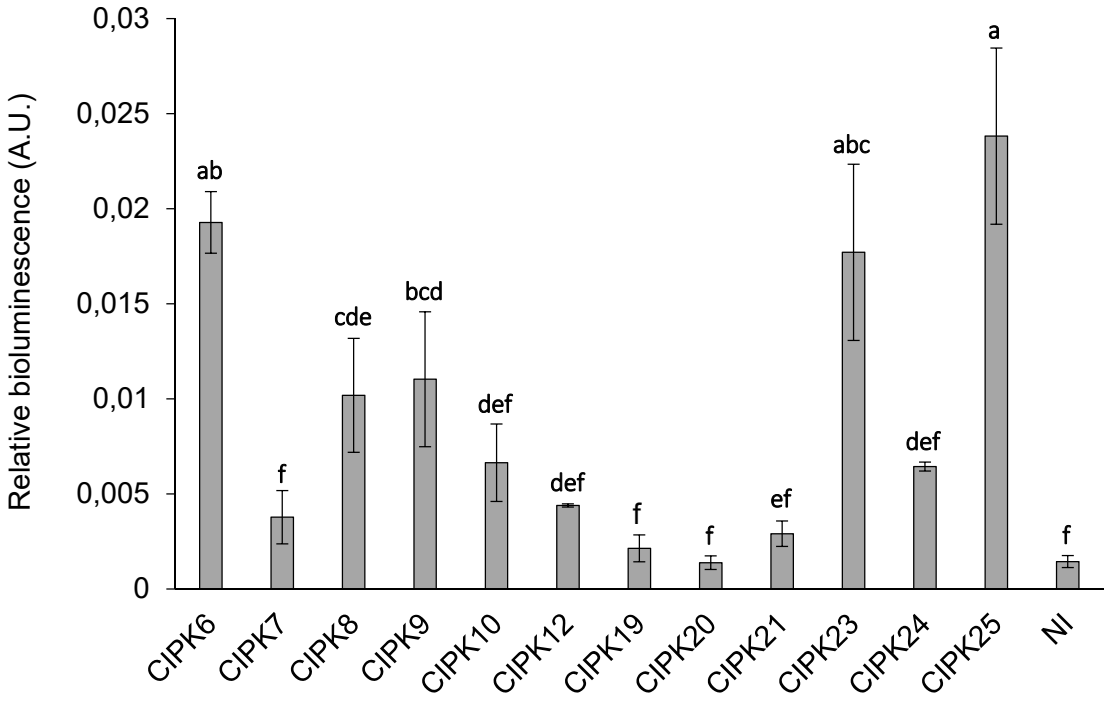

Fig. S1: NRAMP1 and CIPKs split-LUC assay

Relative luminescence in arbitrary units (A.U) obtained by Split-LUC assay between NRAMP1-cLUC and 12 nLUC-CIPKs. Luminescence values were normalized relative to the GFP fluorescence. NI; non infiltrated. Error bars represent ± SD of the mean (n = 3) and different letters indicate significantly different luminescence values (one-way ANOVA, Tukey HSD post-test, $p < 0.05$)

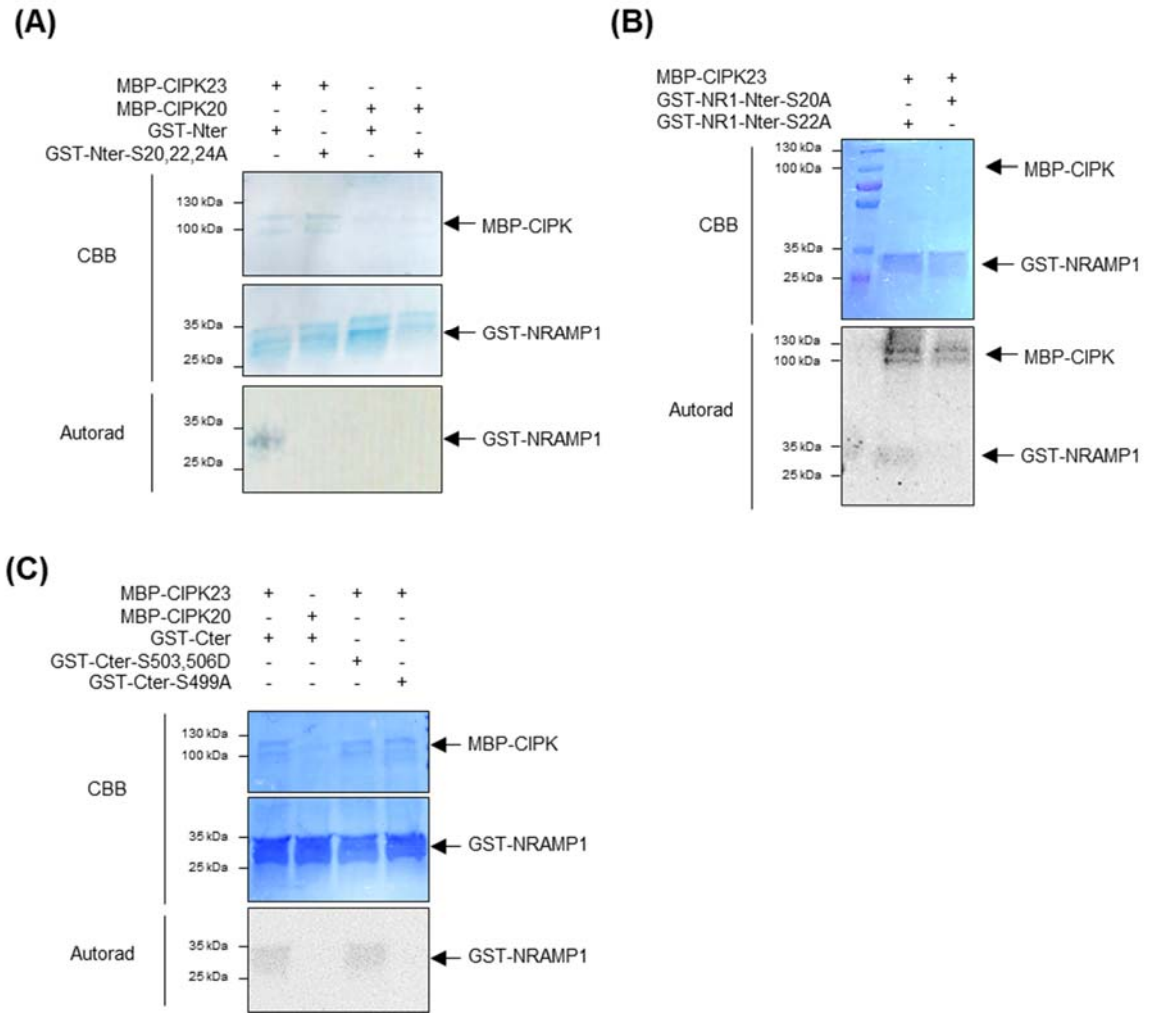

Fig. S2: Biological replicate of Fig 2

(A) *In vitro* phosphorylation assay of N-terminal (GST-Nter) and N-terminal S20,22,24A (GST-Nter-S20,22,24A) regions of NRAMP1 by MBP-CIPK23 or MBP-CIPK20.

(B) *In vitro* phosphorylation assay of N-terminal S20A (GST-Nter-S20A) and N-terminal S22A (GST-Nter-S22A) regions of NRAMP1 by MBP-CIPK23.

(C) *In vitro* phosphorylation assay of C-terminal (GST-Cter), C-terminal S503,506D (GST-Nter-S503,506D) and C-terminal S499A (GST-Nter-S499A) regions of NRAMP1 by MBP-CIPK23 or MBP-CIPK20.

CBB, Coomassie brilliant blue staining. Autorad, autoradiography.

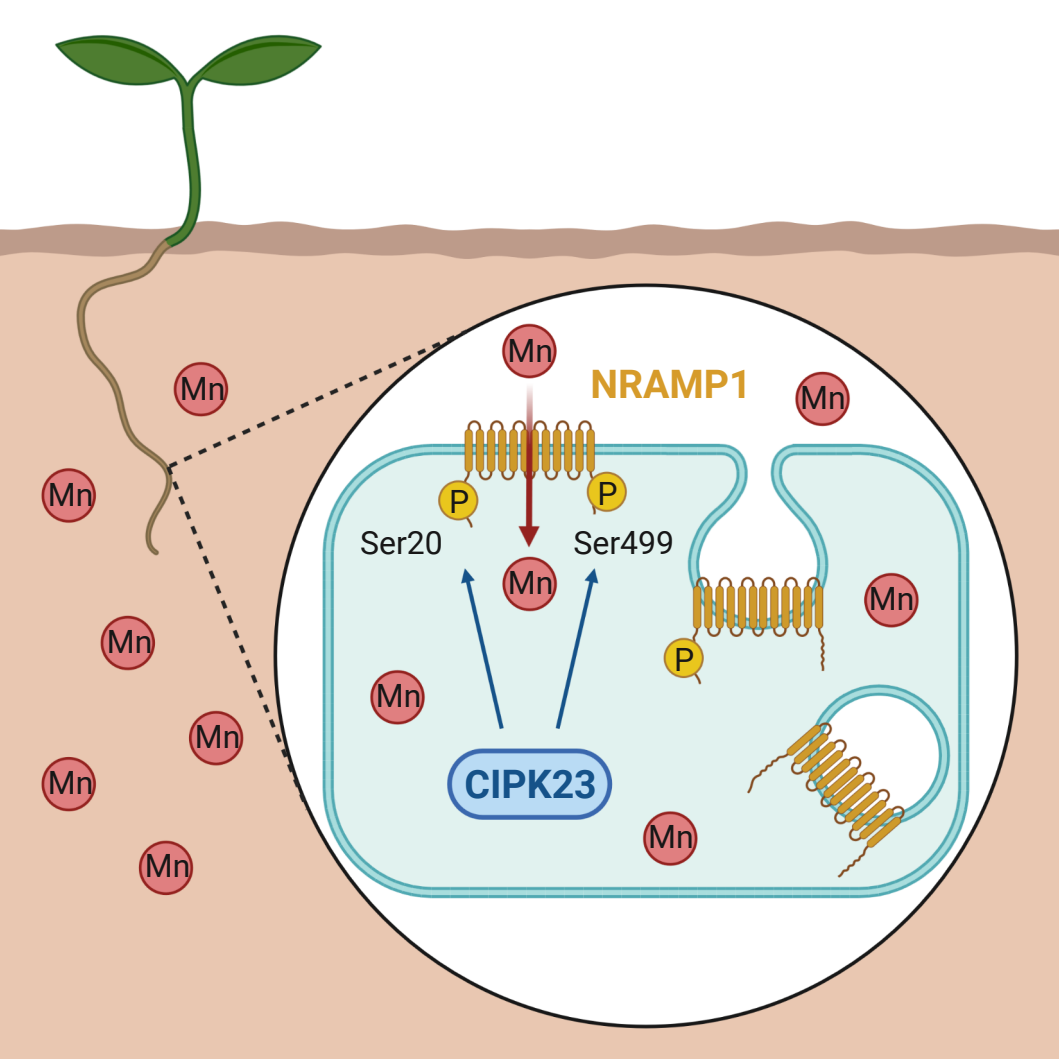
Mn
Mn
Mn
Mn
Mn
Mn
Mn
NRAMP1
Mn
P
P
Ser20
Ser499
Mn
Mn
P
Mn
CIPK23
Mn

Control of manganese uptake in plants relies on the phosphorylation-dependent internalization of the NRAMP1 transporter. Here we show that the calcium-activated kinase CIPK23 interacts with NRAMP1; phosphorylates its serine 20, controlling its endocytosis, and serine 499; and that *cipk23* and *cbl1cbl9* mutations cause plant hypersensitivity to manganese. We discuss how the CBL1/9-CIPK23 module could regulate NRAMP1 in response to Mn availability.